[1] a) R. M. Barrer, *Hydrothermal Chemistry of Zeolites*, Academic Press, New York, **1982**; b) M. E. Davis, *Ind. Eng. Chem. Res.* **1991**, *30*, 1675; c) F. R. Ribeiro, F. Alvarez, C. Henriques, F. Lemos, J. M. Lopes, M. F. Ribeiro, *J. Mol. Catal. A* **1995**, *96*, 245.
[2] R. B. Gennis, *Biomembranes*, *Molecular Structure and Function*, Springer, New York, **1989**, chap. 8, p. 270.
[3] a) J. S. Beck, J. C. Vartuli, R. J. Roth, M. E. Leonowicz, C. T. Kresge, T.-W. Chu, D. H. Olson, *J. Am. Chem. Soc.* **1992**, *114*, 10834; b) C. T. Kresge, M. E. Leonowicz, W. J. Roth, J. C. Vartuli, J. S. Beck, *Nature* **1992**, *359*, 710.
[4] The following review articles are available: a) J. S. Beck, J. C. Vartuli, *Curr. Opin. Solid State Mater. Sci.* **1996**, *1*, 76; b) J. Liu, A. Y. Kim, L. Q. Wang, B. J. Palmer, Y. L. Chen, P. Bruinsma, B. C. Bunker, G. J. Exarhos, G. L. Graff, P. C. Rieke, G. E. Fryxell, J. W. Virden, B. J. Tarasevich, L. A. Chick, *Adv. Colloid Interface Sci.* **1996**, *69*, 131; c) N. K. Raman, M. T. Anderson, C. J. Brinker, *Chem. Mater.* **1996**, *8*, 1682; d) U. Ciesla, F. Schuth, *Microporous Mesoporous Mater.* **1999**, *27*, 131.
[5] K. Möller, T. Bein, *Chem. Mater*. **1998**, *10*, 2950.
[6] a) D. Cauvel, G. Renard, D. Brunel, *J. Org. Chem.* **1997**, *62*, 749; b) S. L. Burkett, S. D. Simms, S. Mann, *Chem. Commun*. **1996**, 1367.
[7] a) L. Mercier, T. J. Pinnavaia, *Adv. Mater*. **1997**, *9*, 500; b) L. Mercier, T. J. Pinnavaia, *Environ. Sci. Technol*. **1998**, *32*, 2749.
[8] a) X. Feng, G. E. Fryxell, L. Q. Wang, A. Y. Kim, J. Liu, K. M. Kemner, *Science* **1997**, *276*, 923; b) J. Liu, X. Feng, G. E. Fryxell, L. Q. Wang, A. Y. Kim, M. Gong, *Adv. Mater.* **1998**, *10*, 161; c) G. E. Fryxell, J. Liu, T. A. Hauser, Z. Nie, K. F. Ferris, *Chem. Mater.* **1999**, *8*, 2148.
[9] M. H. Lim, C. F. Blanford, A. Stein, *Chem. Mater*. **1998**, *10*, 467.
[10] S. Dai, M. C. Burleigh, Y. Shin, C. C. Morrow, C. E. Barnes, Z. Xue, *Angew. Chem.* **1999**, *111*, 1314; *Angew. Chem. Int. Ed.* **1999**, *38*, 1235.
[11] a) S. Inagaki, *J. Am. Chem. Soc*. **1999**, *121*, 9611; b) B. J. Elde, B. T. Holland, C. F. Blanford, A. Stein, *Chem. Mater*. **1999**, *11*, 3302; c) T. Asefa, M. J. MacLachlan, N. Coombs, G. A. Ozin, *Nature* **1999**, *402*, 867.
[12] A. Katz, M. E. Davis, *Nature* **2000**, *403*, 286.
[13] F. H. Dickey, *J. Phys. Chem*. **1955**, *59*, 695.
[14] G. Wulff, B. Heide, G. Helfmeier, *J. Am. Chem. Soc.* **1986**, *108*, 1089.
[15] a) G. Wulff, *Angew. Chem.* **1995**, *107*, 1958; G. Wulff, *Angew. Chem. Int. Ed. Engl.* **1995**, *34*, 1812; b) G. Wulff, A. Sarhan, K. Zabrocki, *Tetrahedron Lett.* **1973**, 4329; c) K. J. Shea, E. A. Thompson, *J. Org. Chem.* **1978**, *43*, 4253; d) D. Spivak, K. J. Shea, *J. Org. Chem.* **1999**, *64*, 4627.
[16] a) G. M. Whitesides, *Sci. Am.* **1995**, *273*(9), 146; b) A. Ulman, *Chem. Rev.* **1996**, *96*, 1533; c) B. C. Bunker, P. C. Rieke, B. J. Tarasevich, A. A. Campbell, G. E. Fryxell, G. L. Graff, L. Song, J. Liu, J. W. Virden, G. L. McVay, *Science* **1994**, *264*, 48.
[17] a) D. Zhao, Q. Huo, J. Feng, B. F. Chmelka, G. D. Stucky, *J. Am. Chem. Soc.* **1998**, *120*, 6024; b) D. Zhao, J. Feng, Q. Huo, N. Melosh, G. H. Fredrickson, B. F. Chmelka, G. D. Stucky, *Science* **1998**, *279*, 548.
[18] a) D. C. Tahmassebi, T. Sasaki, *J. Org. Chem.* **1994**, *59*, 679; b) K. O. Hwang, Y. Yakura, F. S. Ohuchi, T. Sasaki, *Mater. Sci. Eng. C* **1995**, *3*, 137.
[19] B. G. Linsen, A. van den Heuvel in *The Solid Gas Interface*, *Vol. 2* (Eds.: E. A. Flood), Mercel Dekker, New York, **1967**, p. 1025.
[20] M. Kruk, M. Jaroniec, Y. Sakamoto, O. Terasaki, R. Ryoo, C. H. Ko, *J. Phys. Chem. B* **2000**, *104*, 292.
[21] J. N. Israelachvili, *Intermolecular and Surface Forces*, 2nd ed., Academic Press, San Diego, **1992**, p. 99.
[22] F. W. Billmeyer, Jr., *Textbook of Polymer Science*, 3rd ed., Wiley, New York, **1984**, p. 154.
[23] F. A. Carey, R. J. Sundberg, *Advanced Organic Chemistry B: Reactions and Synthesis*, 2nd ed., Plenum, New York, **1983**, p. 57.
[24] E. Angeletti, C. Capena, G. Martinetti, P. Venturello, *J. Chem. Soc. Perkin Trans. 1* **1989**, 105.
[25] a) B. M. Choudary, M. L. Kantam, P. Sreekanth, T. Bandopadhyay, F. Figueras, A. Tuel, *J. Mol. Catal. A* **1999**, *142*, 361; b) I. Rodriguez, S. Iborra, A. Corma, F. Rey, J. L. Jorda, *Chem. Commun.* **1999**, 592.
[26] H. O. House, *Modern Synthetic Reactions*, 2nd ed., W. A. Benjamin, Menlo Park, CA, **1972**, p. 648.

Hierarchical Pore Structures through Diatom Zeolitization**

Michael W. Anderson,* Stuart M. Holmes, Noreen Hanif, and Colin S. Cundy

There has been considerable effort recently to devise routes to hierarchical porous structures, which aid the diffusion of guest species through an inorganic network of pores and channels. In order to optimize the performance of a material for a specific application, it is desirable to combine different levels of porosity into one hierarchical porous material. In applications such as catalysis, where the diffusion of molecules through the pore structure, called "molecular traffic control",[1] is vital for optimum performance, a highly ramified network of macro- and micropores is desired. Further, for bulk processes, again such as catalysis or ion-exchange, then any hierarchical porous material must be both facile and cheap to construct. Herein, we report the use of diatomaceous earth for the controlled synthesis of ordered mesoporous/microporous composites which may have considerable utility for bulk industrial processes.

Diatoms are single-celled algae,[2] microscopic plants which secrete and are enclosed by an intricate silica shell. When these aquatic plants die, their shells collect on the ocean or lake floor, eventually forming the material called diatomaceous earth (kieselguhr) or the more light weight rock called diatomite. Diatomite is used in sound and heat insulation, as filters, abrasives, and in the manufacture of explosives. One unique feature of diatoms is their macroporous channel structure with pore sizes ranging from the submicron to tens of microns scale. As diatoms make up about a quarter of plant life by weight, they are an extremely abundant and cheap source of silica. The purpose of this work is to try to utilize the inherent macroporosity of diatoms in the construction of hierarchical composite materials by their "zeolitization".

Hierarchical pore networks have been predicted for some time to have enhanced diffusion properties, whether the networks are ordered or disordered.[3] Indeed, much of the preparation of working catalyst particles involves the treatment of the active component with a suitable binder (usually a form of clay) such that good diffusion is maintained. However, the control over the level and degree of porosity is somewhat arbitrary and depends upon processing conditions. Recently, elegant efforts to synthesize controlled hierarchical materials have resulted in composites with a pore size distribution spread over up to three orders of magnitude. However, the processing conditions are complicated and

[*] Prof. M. W. Anderson, S. M. Holmes, N. Hanif, C. S. Cundy
UMIST Centre for Microporous Materials
Department of Chemistry
University of Manchester
P.O. Box 88, Manchester M60 1QD (UK)
Fax: (+44) 161-2004527
E-mail: m.anderson@umist.ac.uk

[**] We are grateful to BNFL, BOC, Engelhard, ICI, and EPSRC for financial support and to Richard Plaisted and James Forrest for providing the colloidal silicalite. We would also like to thank Micromeritics Ltd. for their help in obtaining the sorption and porosimetry data.

  1433-7851/00/3915-2707 $ 17.50+.50/0

require the inclusion of latex spheres within the product, which subsequently have to be removed.[4, 5] Alternatively, complex silica forms (mimicking, to some extent, diatoms) have been synthesised using pattern replication of self-organised organic assemblies, such as micelles, vesicles, and foams.[6–8] A "biomimetic" approach to porous materials using a technique called Replamineform[9] has been used to fabricate orthopedic prosthetic devices by deposition of a range of materials[10, 11] on a cast produced from the pore structures of marine invertebrate skeletal materials, such as echinoid spines and coral. However, such forms in themselves do not have suitable active sites for catalysis or ion exchange. In this work, we have developed a simple, cheap, and one-step process to the formation of a stable micro/macroporous composite material where the active component is based upon a zeolite catalyst.

One of the methods we have used to zeolitize the diatomaceous earth involves coating the diatoms with zeolite nanoparticles followed by subsequent attachment and hydrothermal growth of zeolite crystals.[12]

Most diatom shells are essentially composed of silica with traces of other oxides—the diatomaceous earth used in this study contained about 2 wt % alumina. Consequently, these initial studies concentrated on zeolitization with the high-silica zeolite ZSM-5, which in the siliceous limit is called silicalite (both structures belong to the MFI structural type).[13] ZSM-5 is one of the most important commercial zeolites and is used for a wide variety of catalytic transformations including the one-step conversion of methanol into gasoline.[14] The MFI structure consists of a two-dimensional array of intersecting micropores with pore diameter of about 5.5 Å.

Figure 1 shows the progress of diatom zeolitization by X-ray diffraction (XRD). The initial diatom has an XRD pattern which is consistent with the crystalline silica form cristobalite (probably arising from heat treatment during the manufacture of the commercial product). First, silicalite nanoparticles (dimension of approximately 80 nm) are dispersed on the surface of the diatoms and this is followed by a hydrothermal growth process inside an autoclave. The XRD patterns reveal an increase in the intensity of the reflections corresponding to the MFI structure at the expense of the reflections corresponding to cristobalite. The synthesis continued for a total of 72 h.

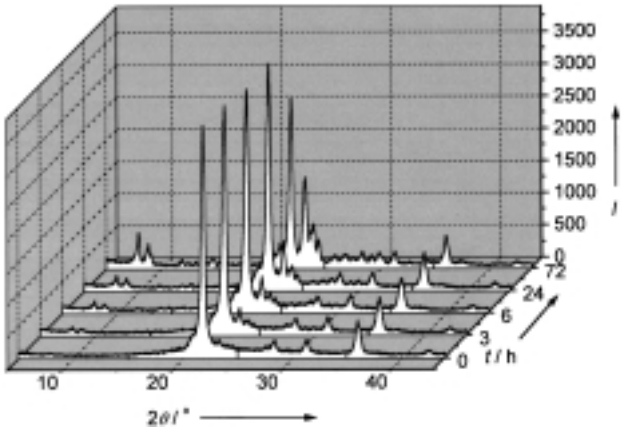

Figure 1. Powder XRD patterns show the development of an MFI phase on the surface of the diatoms. Before growth, the diatoms show reflections characteristic of a cristobalite phase. It is not clear whether the cristobalite phase is homogeneously dispersed through the diatoms or whether parts are essentially amorphous. Electron microscopy shows no indication of opaline regions often associated with diatoms. Subsequent XRD spectra show the growth of reflections characteristic of the MFI phase. The initial nanoparticles are (aluminum free) silicalite. However, an energy-dispersive X-ray spectroscopic (EDAX) analysis of the zeolite layer shows the crystals have about 2% alumina which originates from the low aluminum concentration in the diatoms.

The details of the morphological changes occurring during these growth steps are most clearly revealed by scanning electron microscopy (SEM; Figure 2). The initial diatoms consist of shell forms, which can be described as hollow tubes

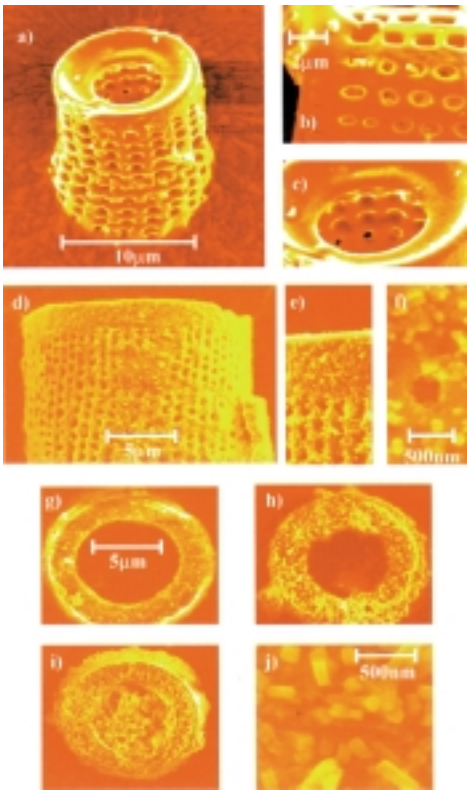

Figure 2. SEM (field emission) of the diatoms before and after growth of the MFI zeolite crystals. a)–c) The parent diatom with overall dimension of about 10×20 μm; in b) the diatom porosity is clearly shown, where the subpores are of dimensions about 0.5 μm. d)–f) The diatoms after 3 h hydrothermal growth. That zeolite nanoparticles are firmly attached is shown in g), by treatment of the same material with boiling water for 1 h. e) The diatom subpores remain free at this stage of hydrothermal growth, and f) the lip of these subpores is lined with nanoparticles. h) After 24 h growth and a calcination step, the interior of the diatoms is still clear and the zeolite nanoparticles have not grown substantially. i), j) After 72 h hydrothermal growth, the interior of the diatoms has become filled with zeolite and the crystals have grown to about 300 nm in length.

of length 15–20 μm and an internal pore diameter of about 4 μm. The walls of the tubes consist of a regular array of submicron pores (about 0.5 μm) with around 0.5 μm of silica between the pores. These pores are continuous into the internal pore space of the hollow diatom tubes. After dispersing the MFI nanoparticles on the diatoms followed by a short subsequent hydrothermal growth step (3 h, Fig-

  1433-7851/00/3915-2708 $ 17.50+.50/0

ure 2d–f), the diatoms have an even coating and the nanoparticles have not grown to any great extent. It is also clear at this stage, that all the macroporosity of the diatoms remains intact (Figure 2g). Further hydrothermal growth (6 h total) enlarges the MFI nanoparticles only slightly. The tube wall openings of the diatom become somewhat restricted but the internal void space remains clear. For up to 24 h, the morphology does not change significantly and the diatom interior remains clear (Figure 2h). However, after 72 h growth, the MFI nanoparticles have grown into typical boat-shaped MFI crystallites of length 300 nm and width 80 nm (Figure 2j). At this stage, it is clear from the electron micrograph that some of the macroporosity of the diatoms is lost, although the basic diatom form remains intact. This image also illustrates the random orientation of the MFI crystals on the surface of the diatoms after 72 h; prior to 72 h, it is not possible to describe the orientation of the crystals since the colloidal seeds appear spherical due to their small size. Most significantly, the internal void space of the diatoms becomes filled with zeolite crystals (Figure 2i).

In order to determine how securely the MFI nanocrystallites are attached to the diatoms, the composite materials after 3 h growth were boiled in water for 1 h followed by examination by SEM. Figure 2g shows that the nanocrystallites are indeed extremely well bound to the diatoms after fixing through short hydrothermal growth steps. The thermal stability of the materials is in excess of 1000 °C and Figure 2h indicates that the composite material is intact after such a treatment. The evolution of the porosity in the composite products was followed by nitrogen sorption/desorption and mercury porosimetry. Whereas the starting material was dominated by macroporosity, zeolite crystal growth introduced a well defined secondary structure that contains both mesopores and micropores. Figure 3 shows the sorption/desorption isotherm for the calcined material which had been

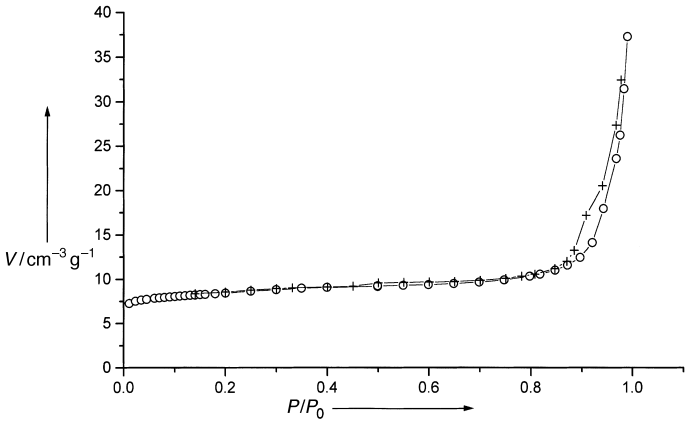

Figure 3. The sorption/desorption isotherm (relative N_2 pressure (P/P_0) against adsorbtion volume (V)) for the calcined material which had been zeolitized for 1 h. ○ desorption, + sorption.

zeolitized for 1 h. This type IV isotherm is indicative of the newly generated porosity in the material, the steep rise followed by the flat section at low relative pressures corresponds to the filling of the micropores (volume 6.7 $cm^3 g^{-1}$ N_2 at STP), while the upturn and hysteresis loop at higher relative pressures reflect the intercrystalline mesoporosity of the zeolitized diatomic structure. The Brunauer-Emmet-Teller (BET) surface area obtained for this material was 29.2 $m^2 g^{-1}$, while the unreacted, calcined, diatomaceous earth had a surface area of only 0.58 $m^2 g^{-1}$ and a micropore volume of 0.13 $cm^3 g^{-1}$. The surface area compares with a value of 421 $m^2 g^{-1}$ given by Stein and co-workers[5] for a macroporous/microporous composite synthesised using latex spheres. The larger surface area in that case is attributable to the higher concentration of zeolite per unit mass of the material. The zeolitized diatom sample had a zeolite content of only about 5% (w/w) at this stage of the reaction. Higher surface area composites can be obtained by zeolitization for longer times.

The diffusion of water through packed columns of the composite materials was tested and compared with that of a packed bed of silicalite crystallites. Figure 4 shows how a very high flow rate is maintained in the composite material.

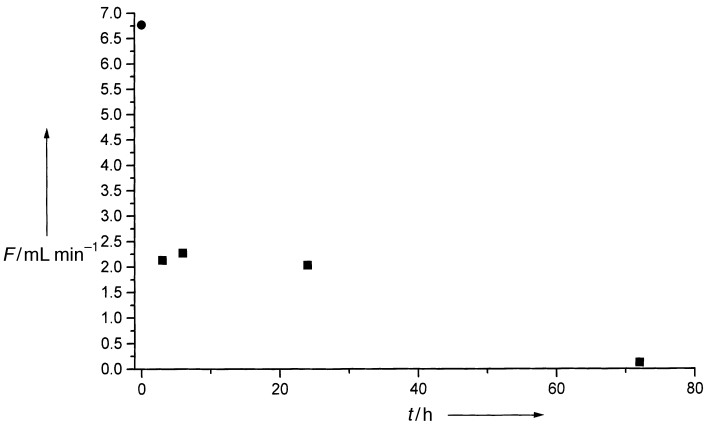

Figure 4. Diffusion rate of water through a packed column at 22 °C. F = flow rate, ● pure diatoms, ■ zeolitized diatoms.

In conclusion, the surface of a diatom structure has been successfully zeolitized to provide a micro/macroporous composite material. One can envisage zeolitizing a range of similar structures, dependent on the physical characteristics of the active bed which are required. As there are over 70000 known diatom species and over 100 zeolite types, the possibility for tailoring both the macroporous and microporous component by this method is almost limitless.

Experimental Section

Diatoms were obtained from Aldrich (Celatom FW80) and used without further treatment. Diatoms were seeded with zeolite nanoparticles (crystallite size about 80 nm) by sonication in a colloidal suspension. This had the effect of fixing the seeds to the surface of the diatoms.[12] The seeded diatoms were then placed in a synthesis mixture of total composition (including the diatoms) SiO_2:Na_2O:EtOH:H_2O:TPABr = 1:0.06:0.43:100:0.04 (TPABr = tetrapropylammonium bromide). A majority (90%) of the silica was provided by the seeded diatoms, the remainder by tetraethyl orthosilicate. The reaction mixture was equilibrated overnight, under stirring, prior to the addition of the seeded diatoms and was then divided between a series of autoclaves and heated to 175 °C.

Received: January 31, 2000 [Z14617]

  1433-7851/00/3915-2709 $ 17.50+.50/0

[1] E. G. Derouane, Z. Gabelica, *J. Catal.* **1980**, *65*, 486.
[2] E. G. Vrieling, T. P. M. Beelen, R. A. van Santen, W. W. C. Gieskes, *J. Biotechnol.* **1999**, *70*, 39.
[3] U. A. El Nafaty, R. Mann, *Chem. Eng. Sci.* **1999**, *54*, 3475.
[4] P. D. Yang, T. Deng, D. Y. Zhao, P. Y. Feng, D. Pine, B. F. Chmelka, G. M. Whitesides, G. D. Stucky, *Science* **1998**, *282*, 2244.
[5] B. T. Holland, L. Abrams, A. Stein, *J. Am. Chem. Soc.* **1999**, *121*, 4308.
[6] S. Mann, G. A. Ozin, *Nature* **1996**, *382*, 313.
[7] H. Yang, N. Coombs, G. A. Ozin, *Nature* **1997**, *386*, 692.
[8] G. A. Ozin, *Chem. Commun.* **2000**, 419.
[9] R. A. White, J. N. Weber, E. W. White, *Science* **1972**, *176*, 922.
[10] J. N. Weber, E. W. White, J. Lebiedzik, *Nature* **1971**, *233*, 337.
[11] D. M. Roy, S. K. Linnehan, *Nature* **1974**, *247*, 220.
[12] S. M. Holmes, C. Markert, R. J. Plaisted, J. O. Forrest, J. R. Agger, M. W. Anderson, C. S. Cundy, J. Dwyer, *Chem. Mater.* **1999**, *11*, 3329.
[13] G. T. Kokotailo, S. L. Lawton, D. H. Olson, W. M. Meier, *Nature* **1978**, *272*, 437.
[14] C. D. Chang, A. J. Silvestri, *J. Catal.* **1977**, *47*, 249.

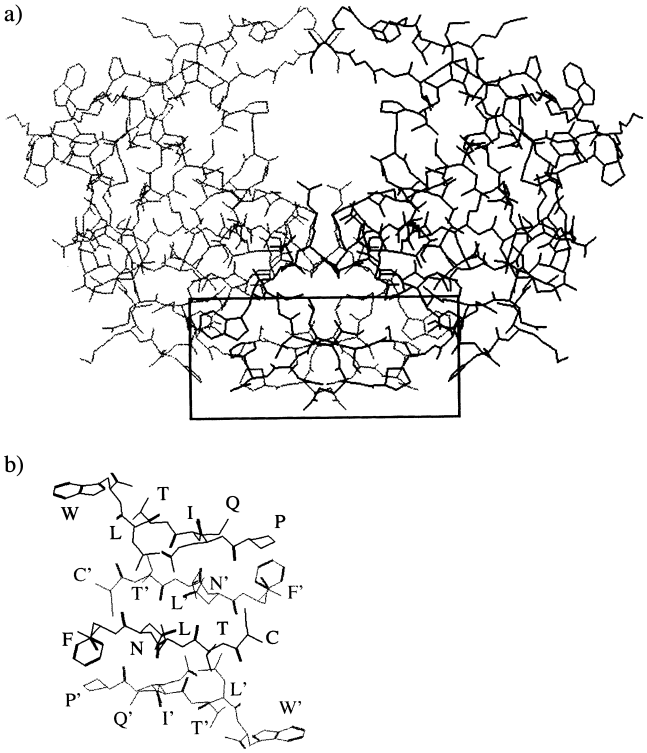

Figure 1. a) Dimeric structure of HIV-1 protease. The area of the N- and C-terminal dimerization interface is indicated by the box. b) The N- and C-terminal dimerization interface of the protease.[10]

Small-Molecule Inhibitors of HIV-1 Protease Dimerization Derived from Cross-Linked Interfacial Peptides**

Michael D. Shultz, Michael J. Bowman, Young-Wan Ham, Xuimin Zhao, George Tora, and Jean Chmielewski*

As more information on macromolecular structure unfolds, it has become obvious that interprotein interactions are a ubiquitous and fundamental aspect of biological activity.[1] Whereas the nature of these protein–protein interactions is becoming better understood, rational approaches to inhibiting these interactions are still in their infancy.[2] Using dimeric HIV-1 protease (Figure 1 a) as a template, we have developed a strategy to inhibit dimerization based on the cross-linking of interfacial peptides derived from the protease.[3] In the current study, we endeavored to identify the essential residues of a cross-linked, interfacial peptide inhibitor of HIV-1 protease, and obtain a minimal structure that maintains the essential features of dimerization inhibition.

The pivotal role of HIV protease in viral replication has made it a prime target for drug design, and there is currently a wide range of potent, active-site inhibitors of HIV-1 protease spanning a number of classes of compounds, including peptide mimetics, C_2-symmetric compounds, and non-peptidic agents.[4] To date five protease inhibitors have been approved by the Food and Drug Administration (FDA) for treatment of HIV infection,[5] but problems of drug resistance due to selection of viruses with specific mutations within protease have been discovered with these inhibitors.[6] Fortunately, results with multidrug approaches made up of protease and reverse transcriptase inhibitors have been promising. Other side effects, however, have also been identified with the current protease inhibitor drugs, including peripheral lipodystrophy,[7] central adiposity,[8] breast hypertrophy in women,[9] hyperlipidemia,[7] and insulin resistance.[7]

The problems that have been identified with the current group of protease inhibitor drugs serve to underscore the need for novel approaches to inhibitor design. One such approach would be to target the dimerization interface of HIV protease.[2] The main dimerization region of HIV-1 protease is found in an interdigitating N- and C-terminal four-stranded, antiparallel β sheet (Figure 1 b).[10] The area centered around the N and C termini accounts for approximately half of the interfacial contact area of the protease homodimer, and the contacts in this area account for greater than 75 % of the free energy of dimerization.[11] This region is also highly conserved among HIV-1 isolates and some HIV-2 isolates, presumably due to the fact that a mutation in the C terminus would necessitate a concomitant mutation in the N terminus to avoid loss of high-affinity dimerization.[12]

Taking advantage of the dimeric nature of HIV protease, Craik and co-workers developed mutant forms of HIV protease for use in a dominant-negative strategy of inhibition; incubation of wild-type protease with monomers that have mutated active-site residues (fourfold molar excess) led to

[*] Prof. J. Chmielewski, M. D. Shultz, M. J. Bowman, Y.-W. Ham, X. Zhao, G. Tora
Department of Chemistry
Purdue University
West Lafayette, IN 47907 (USA)
Fax: (+1) 765-494-0135
E-mail: chml@purdue.edu

[**] This work was supported by NIH (GM52739) and NSF (9457372-CHE).

Supporting information for this article is available on the WWW under http://www.wiley-vch.de/home/angewandte/ or from the author.

  1433-7851/00/3915-2710 $ 17.50+.50/0